Available online at www.sciencedirect.com

SciVerse ScienceDirect

Ceramics International 39 (2013) 6623–6629

CERAMICS INTERNATIONAL

www.elsevier.com/locate/ceramint

Enhancement of piezoelectric and ferroelectric properties of $BaTiO_3$ ceramics by aluminum doping

Ahmed I. Ali[a,b], Chang Won Ahn[a], Yong Soo Kim[a,*]

[a]Energy Harvest–Storage Research Center and Department of Physics, University of Ulsan, Ulsan 680-749, South Korea
[b]Basic Science Department, Faculty of Industrial Education, Helwan University, Saray El-Quba, Cario 11281 Egypt

Received 15 December 2012; received in revised form 28 January 2013; accepted 28 January 2013
Available online 5 February 2013

Abstract

Ferroelectric and piezoelectric properties of $BaTiO_3$ and Al-doped $BaTiO_3$ ceramics were investigated. The ferroelectric study demonstrated that, by doping Al^{3+} ions in the A-site of $BaTiO_3$, the polarization–electric field loop exhibited enhanced remnant polarization (from 12 to 17.5 $\mu C/cm^2$), saturation and switching. In addition, the piezoelectric constant (d_{33}) increased with Al-doping for both static and dynamic strain values (from 75 to 135 and from 29.2 to 57.9 pC/N, respectively, at a maximum applied electric field of 16 kV/cm). Furthermore, the dielectric constant values increased and both the dielectric loss factor and leakage current decreased, even though the transition temperature shifted to lower temperature (from 121 to 113 °C) for the Al-doped sample. Therefore, the Al-doped $BaTiO_3$ has adjustable piezoelectric and ferroelectric properties.

Keywords: C. Dielectric properties; Doping effect; Ferroelectric; Ferroelectric ceramics; Piezoelectric

1. Introduction

Of late, attention is being given to some ferro-piezoelectric materials due to the requirements to develop high piezoelectric sensitivity and lead-free compositions of ferro-piezoelectric ceramics [1–3]. Piezoelectric materials are used in sensor and actuator technologies because of their ability to couple electrical and mechanical displacements, resulting in electrical polarization changes in response to applied mechanical stress and/or strain that can generate an electric field [4]. The development of high piezoelectric sensitivity and lead-free composition materials remains a major scientific challenge, driven by both the toxicity of lead oxide (PbO) and directives for environmental protection. Such directives require the elimination of PbO from the composition of ferro-piezoelectric ceramics in devices.

$BaTiO_3$ (BT), a member of a large family of perovskite compounds with the general formula of ABO_3 [5], is the first ferroelectric/piezoelectric ceramic and a good candidate for a variety of applications due to its excellent dielectric, ferroelectric and piezoelectric properties. However, BT exhibits a relatively low Curie temperature (T_c), which results from the ferroelectric tetragonal to paraelectric cubic phase transition at 120 °C [6]. Recent reports of BT materials have investigated physical properties, including piezoresistivity [7], colossal permittivity up to 10^6 in carefully prepared nanocrystalline ceramics [8], and high reversible strain up to ~0.8% due to defect-mediated domain switching [9]. The doping role in the BT properties is very complex and not fully understood. The addition of a dopant usually changes more than one property. For example, the addition of Y_2O_3 flattens the T_c of BT, but lowers the maximum permittivity and changes the grain growth [10]. For special industrial applications, one feature is changed with the amount of dopant. When $BaTiO_3$ is doped with an acceptor, oxygen vacancies are formed to maintain charge neutrality. However, the formed conduction electrons are trapped by the acceptor dopants, and the semiconductor behavior is concealed. Common acceptor dopants used in BT ceramics include Co^{2+} [11,12], Ca^{2+} [13], Cr^{3+} [14], Mn^{2+} [14–16], and Mg^{2+} [15–17]. Jeong and Hand [16] reported that the leakage current of MnO

*Corresponding author. Tel.: +82 522592326.
E-mail address: yskim2@ulsan.ac.kr (Y.S. Kim).

0272-8842/$ - see front matter © 2013 Elsevier Ltd and Techna Group S.r.l. All rights reserved.
http://dx.doi.org/10.1016/j.ceramint.2013.01.099

and MgO acceptor-doped BT was effectively suppressed by co-doping. The reduced leakage current may be ascribed to the change of Mn ions from bivalent to trivalent/tetravalent states with increasing oxygen partial pressure and change in microstructure. Lee et al. [18] demonstrated that the addition of Al^{3+} at the B-site can reduce the maximum temperature (T_m) of the phase transition in BT. There are a few studies on the ferro-piezoelectric properties of Al-doped BT, which is valuable for some ceramic applications.

In this work, $BaTiO_3$ and $Al_{0.01}Ba_{0.99}TiO_3$ ceramic samples were synthesized, and the structural, ferro-piezo-dielectric properties were characterized. Based on the experimental data, Al-doped $BaTiO_3$ exhibited enhanced piezoelectric and ferroelectric properties.

2. Experiments

$BaTiO_3$ and $Al_{0.01}Ba_{0.99}TiO_3$ ceramic samples were prepared by a conventional powder processing method. Powders of all chemicals, TiO_2 (99.99%), $BaCO_3$ (99.9%), and Al_2O_3 (99.99%), were obtained from Aldrich. The powders were mixed in an ethanol medium with zirconia balls by stirring in a high-speed turbine at 5000 rpm for 36 h. The slurry was dried at 120 °C in an oven. Mixtures were crushed into a powder, ground lightly in an agate mortar and sieved through a 100 μm mesh screen. The obtained powder was fired at 1100 °C for 8 h. This process was repeated twice, and the powder was then molded into a pellet (2.5 cm length, 2.5 cm width and 3 mm thickness) under a uni-axial pressure of 12 MPa. Cold-iso-static pressing was performed under 150 MPa for 10 min. The samples were sintered in oxygen at 1350 °C for 48 h.

The microstructures of ceramic samples were analyzed with field emission scanning electron microscopy (FE-SEM; JEOL, JSM-65OFF) and X-ray powder diffraction (XRD, Rigaku Co-Miniflex X-ray diffractometer employing CuK_α radiation with $\lambda = 0.15418$ nm). For ferroelectric (P–E loops) measurements with a parallel-plate capacitor configuration, Ag-paste was applied to both polishing surfaces of the sintered disk and the electrodes were formed by heating in a 100 °C furnace for 10 min. The hysteresis loops were measured using a Sawyer–Tower circuit up to a maximum electric field of 60 kV/cm with an applied voltage of a triangular waveform [19]. The induced strain according to applied electric field was measured using a linear variable differential transducer (LVDT; MCH-331 and M401, Mitutoyo). The voltage was supplied using a high voltage amplifier (610E, TREK) derived by a waveform generator (33250A, Agilent).

The piezoelectric properties were measured using a Berlincourt meter after poling the samples with an electric field of 3 kV/mm for 10 min at 80 °C. The electric polarization (P) as a function of the mechanical strain (S) at different applied electric fields (E) was measured in a silicon oil bath using a modified Sawyer–Tower circuit and an LVDT. The static piezoelectric coefficient (d_{33}) was measured by a direct method based on a ZJ-3AN Quasi-static d_{33}-meter using the Berlincourt method. Normalized strain ($d^*_{33} = S_{max}/E_{max}$) was calculated from the ratio of the maximum strain to the maximum electric field from the unipolar strain curves. The specimens for the piezoelectric measurements were disks with 3.05×2.04 and 1.96×2.33 mm^2 areas and 1.24 and 1.02 mm thickness for the $BaTiO_3$ and Al–$BaTiO_3$ ceramics, respectively. The dielectric constant and tangent loss of the samples as a function of temperature were measured in the frequency range of 10–10^6 Hz using an impedance analyzer (HP4192) attached to a programmable furnace. This measurement was performed in air over 30–400 °C using a homemade furnace (heating/cooling rate of 0.6 °C/min). The electrical current–voltage measurement was performed at room temperature with a Keithley 2636A.

3. Results and discussion

Fig. 1(a) depicts the XRD pattern at room temperature. The analysis of XRD patterns of BT clearly indicated that the synthesized sample was a single phase (cubic structure) and all reflections corresponded to BT without residuals of

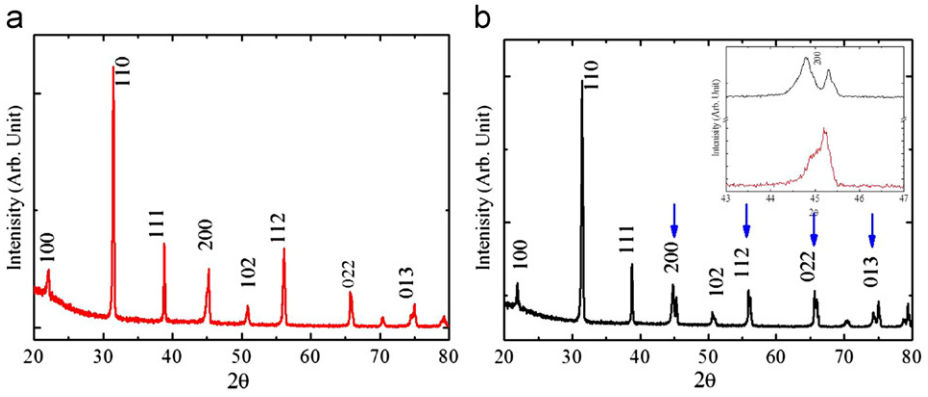

Fig. 1. X-ray diffraction (XRD) patterns of (a) $BaTiO_3$ and (b) $Al_{0.01}Ba_{0.99}TiO_3$ ceramics measured at room temperature. The inset in (b) shows the peak splitting of the cubic to tetragonal structure.

the original constituent oxides [20]. The lattice parameter fitted with powder cell software was 3.8327 Å (JCPDS 83-1880). Fig. 1(b) presents the XRD patterns of the ABT ceramic. The formation of a pure $BaTiO_3$ phase was confirmed during the calcination stages, indicating that Al^{3+} diffuses into the lattice site of the $BaTiO_3$ ceramic, forming a solid solution. The Al-doped sample has more than four peaks of principal perovskite reflections. The XRD data is well fitted to the tetragonal phase (a=3.9889 Å, c=4.0232 Å and a/c=0.9915), showing that the Al^{3+} ions cause a structure distortion from the cubic to tetragonal phase. According to Cui et al. [21], the Al ions can substitute into the B-sites of $BaTiO_3$, resulting in the formation of new compounds or intermediates, such as hexagonal $BaAl_2O_4$ or monoclinic $Ba_4Ti_{10}Al_2O_{27}$ phases if the content of Al is greater than 0.02. In our case, the Al-content was 0.01 mol in the A-site doping. Therefore, the Al substitution at the A-site can increase the doping level of Ti at the B-site. Though the ionic radius of Al^{3+} (0.62 Å) is close to that of Ti^{4+} (0.67 Å) and smaller than that of Ba^{2+} (1.56 Å), the large mismatch of the A-site cation plays the dominant role in decreasing the lattice parameters, and the resulting distortion of the crystal structure contributed to the Al-doped sample in $BaTiO_3$.

Fig. 2 presents the FE-SEM images of both $BaTiO_3$ and Al-$BaTiO_3$ ceramic samples. The average grain size increased from approximately 0.5 μm to approximately 1.4 μm with the addition of the Al^{3+} element. The Al^{3+} element in $BaTiO_3$ ceramics can increase the ferroelectric domain wall and the grain size, further inducing the defects and homogeneity of the $BaTiO_3$ ceramic. This behavior may be due to an oxygen vacancy because the samples were sintered at high temperature (1350 °C) and in an oxygen environment. The sintering history with metal in the dielectric caused the Al ions to dissolve well in the $BaTiO_3$.

Measurement of the P–E hysteresis loops was performed to examine the ferroelectric properties of $BaTiO_3$ and $Al_{0.01}Ba_{0.99}TiO_3$ ceramics. Fig. 3(a) shows the P–E hysteresis loops of BT and ABT ceramic samples. The remanent polarizations, P_r, were 11.4 and 5 μC/cm^2, while the coercive fields, E_c, were 4 and 3.1 kV/cm for ABT and BT ceramics at a maximum applied field of 16 kV/cm, respectively. Both undoped and Al-doped samples saturated with coercive fields (E_c) had nearly the same polarization (~4 kV/cm). Thus, the replacement of the Ba^{2+} ion by Al^{3+} in the A-site of BT can enhance the polarization, which may be originally generated from an increase in the polarized domain wall size and domain ordering during the electric poling sequence. However, the ferroelectric property for the ABT ceramic was better than that of the BT ceramic.

The leakage current characteristics of the BT and ABT ceramics were also investigated. Fig. 3(b) shows the current density as a function of applied electric fields for the Pt/$Al_{0.01}Ba_{0.99}TiO_3$/Pt and Pt/$BaTiO_3$/Pt ceramic capacitors. The current density for the ABT ceramic decreased compared to that of the BT, suggesting that the ABT ceramic quality was improved and was better than that of the BT ceramics. Therefore, the A-site doping of ferroelectric perovskite enhances the ferroelectric characteristics and leakage currents. In addition, the doping decreased the leakage current density by approximately 50% due to the decreasing ionic current by doping with Al^{3+} but increased local capacitance induced by Al^{3+} and $BaTiO_3$ ions. Furthermore, the total capacitance increases in dielectric measurements. Table 1 shows the piezoelectric properties, such as the planar electromechanical coupling factor (k_p) and piezoelectric constant (d_{33}), at room temperature for the BT and ABT ceramics. k_p and d_{33} increased more for Al-doped than undoped ceramic samples. According to the thermodynamic theory of ferroelectrics [22], the increase in these parameters is acceptable because d_{33} and k_p can be expressed as

$$d_{33} = 2Q_{11}P_r\varepsilon_{33}^T \tag{1}$$

$$k_p = \frac{2Q_{12}P_r}{(1-E)(\varepsilon_{33}^T/S_E)} \tag{2}$$

respectively, where Q_{11} and Q_{12} represent the electrostrictive coefficients that are constants for the perovskite material; P_r, ε_{33}^T, S_E and E represent the remanent polarization, the dielectric constant of the poled sample, the elastic compliance coefficient and Poisson's ratio,

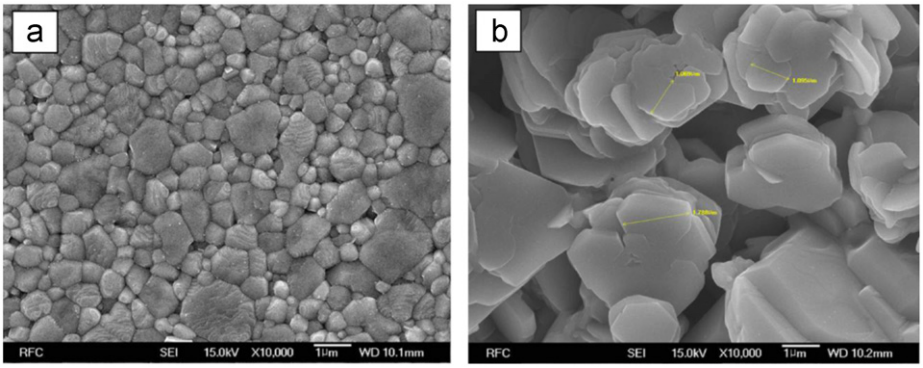

Fig. 2. FE-SEM micrographs of (a) $BaTiO_3$ and (b) $Al_{0.01}Ba_{0.99}TiO_3$ ceramics sintered in oxygen at 1350 °C for 48 h.

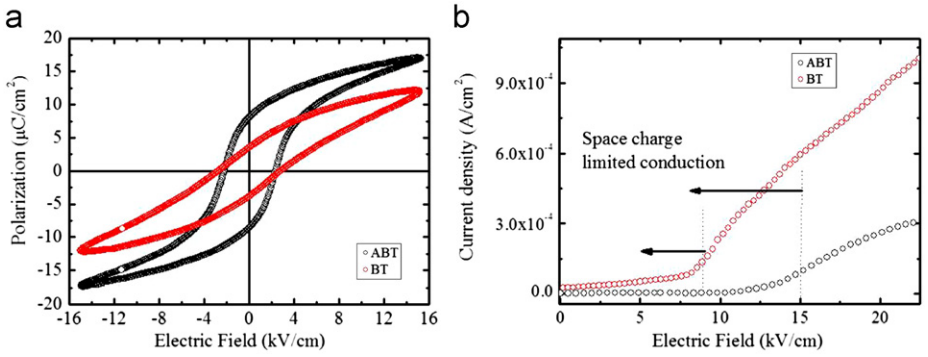

Fig. 3. (a) *P–E* hysteresis loops and (b) current density as a function of electric field of $BaTiO_3$ and $Al_{0.01}Ba_{0.99}TiO_3$ ceramics.

Table 1
Planar electromechanical coupling factor (k_p), normalized strain (d^*_{33}) and piezoelectric constant (d_{33}) at room temperature and the Curie temperature for $BaTiO_3$ (BT) and $Al_{0.01}Ba_{0.99}TiO_3$ (ABT) ceramics.

Sample	k_p	Normalized strain (d^*_{33})	d_{33} (pC/N)	Grain size (μm)	T_c (°C)
BT	1.86	29.15	75	0.5	126
ABT	1.53	57.58	135	1.38	113

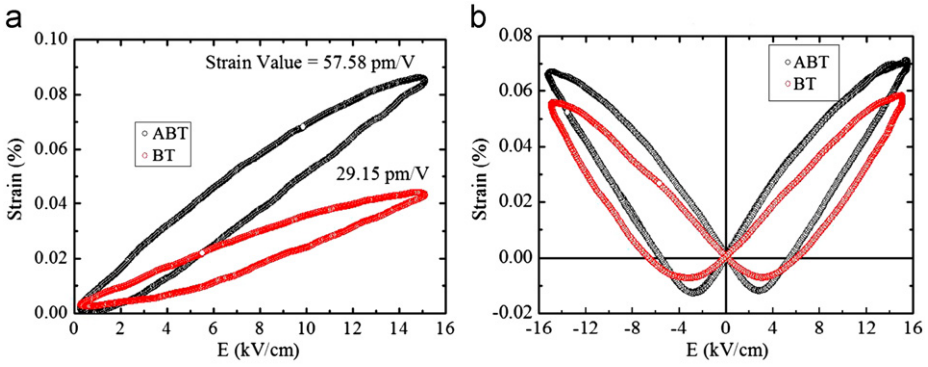

Fig. 4. (a) Unipolar *S–E* hysteresis loops and (b) bipolar *S–E* hysteresis loops of $BaTiO_3$ and $Al_{0.01}Ba_{0.99}TiO_3$ ceramics.

respectively. d_{33} and k_p are proportional to P_r, and therefore, an increase in P_r results in an increase in d_{33} and k_p.

Fig. 4(a) shows the unipolar field-induced strains of BT and ABT ceramics. Strains of 0.085% and 0.042% corresponding to d_{33} values of 57.58 pm/V and 29.15 pm/V, respectively, were obtained for the ABT and BT ceramics at an applied electric field of 16 kV/cm. The unipolar strain of ABT was twice as large as that of BT. A brief comparison of ABT with the BT ceramic data was drawn and is shown in Fig. 4 and Table 1, suggesting that ABT ceramics are a promising lead-free alternative material for electromechanical actuator applications. The enhanced field-induced strain and corresponding d_{33} are due to the partial substitution by Al^{3+} of ionic radius 0.67 Å, which is smaller than the Ba^{2+} ionic radius (1.49 Å) and may cause a local distortion in the crystal structure of the BT ceramic [23]. Cui et al. [21] and Takenaka et al. [24] observed a high strain response for a $K_{0.5}Na_{0.5}NbO_3$-modified $Bi_{0.5}Na_{0.5}TiO_3$–$BaTiO_3$ system and concluded that the large strain is originally due to the presence of a non-polar dielectric phase that changed the system and returned to the unpoled state upon removing the applied electric field, which led to a large unipolar strain. Similarly, the high strain response in the $Al_{0.01}Ba_{0.99}TiO_3$ ceramic sample may be associated with the coexistence of ferroelectric and non-polar phases induced by Al-substitution.

Fig. 4(b) shows the bipolar field-induced strains of the BT and ABT ceramics. The bipolar strain also increased from 0.055% to 0.068% at an applied electric field of 16 kV/cm for BT and ABT ceramics, respectively. The BT and ABTB ceramics exhibited a ferroelastic order, i.e., a typical butterfly-shaped curve was exhibited with a negative strain (S_n) of 0.012% and 0.01% for BT and ABT ceramics, respectively. However, the Al-modified BT showed a symmetric curve, i.e., a more ideal shape and adjustable form than those of the undoped BT. This behavior can be attributed to doping by

Al ions, which increased the number of local nano-capacitors in the sample and was reflected in the ferroelectric and dielectric properties.

The dielectric constant (ε') and loss (tan δ) as a function of the temperature at different applied frequencies (1, 10, 100 and 1000 kHz) are presented in Figs. 5 and 6, respectively. A dielectric anomaly was observed in the dielectric curves of the BT and ABT ceramics at 123 and 113 °C, respectively. The anomaly is related to the structural phase transition from the tetragonal phase to the cubic phase of $BaTiO_3$. The high dielectric constant of barium titanate below T_c is due to the permanent dipole in the structure. At T_c, the high dielectric constant value is due to the increasing mobility of Ti^{4+} ion dipoles and the unstable lattice structure in the vicinity of phase transitions. The T_c shifted to a lower temperature with Al doping, but the dielectric constant slightly increased. In addition, the dielectric loss decreased for the Al-doped $BaTiO_3$ ceramic. Generally, the increasing dielectric constant is related to the domain alignment and domain structure. The shift of T_c to a lower temperature in the Al-doped $BaTiO_3$ ceramic may be due to the increasing ferroelectric order induced by the Al ions. Recently, a similar behavior of Zr–$BiNaKTiO_3$ was observed by Hussain et al [19]. Moreover, the influences of doping at the A-site on the dielectric properties of $BaTiO_3$ ceramics are in adherence to the corresponding rules of ceramics. As a result, doping of the A-site leads to the enhanced piezoelectric constant, followed by decreased dielectric constant and loss tangent, which is similar to those of PZT-based ceramics with Nb^{5+} doping as a soft additive [25].

It is commonly reported [14,16,26] that the dielectric constant of barium titanate is dependent on the grain size of the ceramic. A maximum dielectric constant is observed for grain sizes of 0.6–1.0 μm. With decreasing grain size, the dielectric constant drops significantly. Mostaghaci and Brook [27] state that this is due to the disappearance of unit cell tetragonality and the multi-domain structure. The phenomenon concerning this dependency on the grain size of the dielectric constant is called the grain size effect, which means that the replacement of the Ba ion with the Al ion can increase the dielectric dipoles between Al ions in the A-site and Ti ions in the B-site of the perovskite lattice. The coupling between Al ions and Ti ions can enhance the ferroelectric property due to the dipole interaction between Ti^{3+} and Ti^{4+}, which was observed in perovskite systems [2,5,11,26]. By simple comparison, $Al_{0.01}Ba_{0.99}TiO_3$ has the greatest E_c, P_r, d_{33} and ε values. In addition, both the dielectric loss and leakage current are reduced by Al doping, which are corroborated with the observation that the ABT has a large grain size (Fig. 2) compared to BT. Since the ferroelectricity is strongly dependent on the interaction between neighboring dipoles, an increase in the grain size (or domain) can align dipoles and increase the ferroelectricity. Thus, the high domain wall energy induced by Al^{3+} doping simultaneously

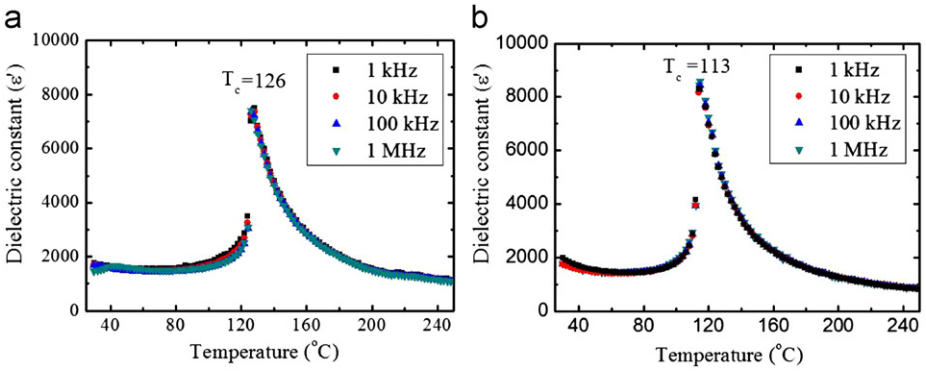

Fig. 5. Dielectric constant as a function of temperature of (a) $BaTiO_3$ and (b) $Al_{0.01}Ba_{0.99}TiO_3$ ceramics with different applied frequencies.

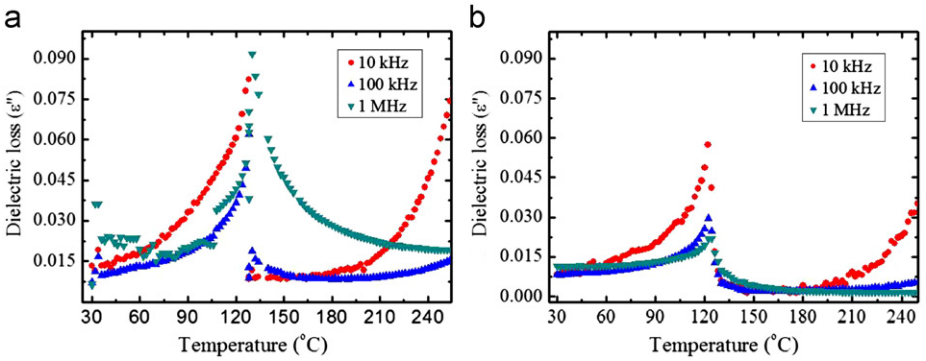

Fig. 6. Dielectric loss as a function of temperature of (a) $BaTiO_3$ and (b) $Al_{0.01}Ba_{0.99}TiO_3$ ceramics with different applied frequencies.

enhances the ferroelectric characteristics, leakage currents, and piezoelectricity.

Based on the interpretation of the enhanced ferroelectric properties of the $BaTiO_3$ ceramic by Al-doping during the application of an electric field, it is possible to create periodic domain patterns with significantly increased charged domain walls with increasing domain-wall density [7,8]. When the domain period increased to several micrometers, the built-in field can lead to enhanced ferroelectric and piezoelectric responses of the poly-domain structure. Another important factor is the role of the Al ions as conductive plates for small capacitors working locally in the ABT sample, which increases the total capacitance of the sample. In addition, Al may increase the ferroelectricity and dielectric constant. Alternatively, doping the $BaTiO_3$ ceramic with Al^{3+} ions decreased the dielectric loss and leakage current. The domain size in BT ceramics is strongly influenced by the domain structure in neighboring grains, both with regard to domain wall spacing and orientation [28].

4. Conclusion

The influences of Al^{3+} doping on the ferroelectric–piezoelectric properties of $BaTiO_3$ ceramics were investigated. The XRD and FE-SEM analysis at room temperature has shown that BT and ABT ceramics existed in cubic and tetragonal phase structures, respectively. ABT showed enhanced static and dynamic piezoelectric constants (d_{33}), unipolar and bipolar strains, and curve shapes. In addition, P–E hysteresis loops showed that the Al-doped sample had a larger polarization remanent, P_r, and smaller coercive field, E_c, than those of pure $BaTiO_3$. Furthermore, the dielectric constant increased and the dielectric loss factor and leakage current decreased. However, T_c slightly shifted to a lower temperature for the Al-doped sample. The addition of 1.0 mol% of Al^{3+} ions in the A-site improved and adjusted the ferroelectric and piezoelectric properties of the $BaTiO_3$ ceramic. A theoretical, detailed study on the Al-doped $BaTiO_3$ ceramic is required to understand the role of Al-doping and its effect on the physical properties.

Acknowledgments

This research was supported by the Leader Industry–University Cooperation (LINC) Project, Basic Science Research Program (2012-1010369) and Priority Research Centers Program (2009-0093818) through the National Research Foundation of Korea (NRF) funded by the Ministry of Education, Science and Technology (MEST).

References

[1] G.H. Haertling, Ferroelectric ceramics: history and technology, Journal of the American Ceramic Society 82 (1999) 797–818.
[2] Y. Saito, H. Takao, T. Tani, T. Nonoyama, K. Takatori, T. Homma, T. Nagaya, M. Nakamura, Lead-free piezoceramics, Nature 432 (2004) 84–87.
[3] J. Rödel, A.B.N. Kounga, M. Weissenberger-Eibl, D. Koch, A. Bierwisch, W. Rossner, M.J. Hoffmann, R. Danzer, G. Schneider, Development of a roadmap for advanced ceramics, Journal of the European Ceramic Society 29 (2009) 1549–1560.
[4] M. Alguero, B.L. Cheng, F. Guiu, M.J. Reece, M. Poole, N. Alford, Ferroelectric hysteresis loops of (Pb,Ca)TiO_3 thin films under spherical indentation, Journal of the European Ceramic Society 21 (2001) 1437–1440.
[5] J. Yao, C. Xiong, L. Dong, C. Chen, Y. Lei, L. Chen, R. Li, Q. Zhu, X. Liu, Enhancement of dielectric constant and piezoelectric coefficient of ceramic–polymer composites by interface chelation, Journal of Materials Chemistry 19 (2009) 2817–2821.
[6] S. Wada, S. Suzuki, T. Noma, T. Suzuki, M. Osada, M. Kakihana, S.E. Park, L.E. Cross, T.R. Shrout, Enhanced piezoelectric property of barium titanate single crystals with engineered domain configurations, Japanese Journal of Applied Physics 38 (1999) 5505–5511.
[7] J.S. Capurso, W.A. Schulz, Piezoresistivity in PTCR barium titanate ceramics I: experimental findings, Journal of the American Ceramic Society 81 (1998) 337–346.
[8] S. Guillemet-Fritsch, Z. Valdez-Nava, C. Tenailleau, T. Lebey, B. Durand, J.Y. Chane-Ching, Colossal permittivity in ultrafine grain size $BaTiO_{3-x}$ and $Ba_{0.95}La_{0.05}TiO_{3-x}$ materials, Advanced Materials 20 (2008) 551–555.
[9] X.B. Ren, Large electric-field-induced strain in ferroelectric crystals by reversible domain switching, Nature Materials 3 (2004) 91–94.
[10] Y.H. Song, J.H. Hwang, Y.H. Han, Effects of Y_2O_3 on temperature stability of acceptor-doped $BaTiO_3$, Japanese Journal of Applied Physics 44 (2005) 1310–1313.
[11] X. Zhou, S. Zhang, Y. Yuan, D. Li, J. Liu, Preparation of $BaTiO_3$-based nonreducible X7R dielectric materials via nanometer powders doping, Journal of Materials Science: Materials in Electronics 17 (2006) 133–136.
[12] M.N. Rahaman, R. Manaler, Grain boundary mobility of $BaTiO_3$ doped with aliovalent cations, Journal of the European Ceramic Society 18 (1998) 1063–1071.
[13] T. Mazon, A.C. Hernandes, A.G. Souza Filho, A.P.A. Moraes, A.P. Ayala, P.T.C. Freire, J. Mendes Filho, Structural and dielectric properties of Nd^{3+}-doped $Ba_{0.77}Ca_{0.23}TiO_3$ ceramics, Journal of Applied Physics 97 (2005)104113-104117 97 (2005).
[14] X.H. Wang, X.Y. Deng, H.L. Bai, H. Zhou, W.G. Qu, L.T. Li, I.W. Chen, Two-step sintering of ceramics with constant grain-size II: $BaTiO_3$ and Ni–Cu–Zn ferrite, Journal of the American Ceramic Society 89 (2006) 438–443.
[15] C.-S. Chen, C.-C. Chou, I.-N. Lin, Microstructures of X7R type base-metal-electroded $BaTiO_3$ capacitor materials prepared by duplex-structured process, Journal of the European Ceramic Society 25 (2005) 2743–2747.
[16] J. Jeong, Y.H. Hand, Electrical properties of acceptor doped $BaTiO_3$, Journal of Electroceramics 13 (2004) 549–553.
[17] W.C. Yang, C.T. Hu, I.N. Lin, Effect of Y_2O_3/MgO co-doping on the electrical properties of base-metal-electroded $BaTiO_3$ materials, Journal of the European Ceramic Society 24 (2004) 1479–1483.
[18] S.J. Lee, S.M. Park, Y.H. Han, Dielectric relaxation of Al-doped $BaTiO_3$, Japanese Journal of Applied Physics 48 (2009) 031403–031407.
[19] A. Hussain, C.W. Ahn, J.S. Lee, A. Ullah, I.W. Kim, Large electric-field-induced strain in Zr-modified lead-free $Bi_{0.5}(Na_{0.78}K_{0.22})_{0.5}TiO_3$ piezoelectric ceramics, Sensors and Actuators A: Physical 158 (2012) 84–89.
[20] E.E. Oren, A.C. Tas, Hydrothermal synthesis of Dy-doped BaTiO3 powders, Metallurgical and Materials Transactions 30B (1999) 1089–1093.
[21] L. Cui, Y.D. Hou, S. Wang, C. Wang, M.K. Zhu, Relaxor behavior of (Ba,Bi)(Ti,Al)O_3 ferroelectric ceramic, Journal of Applied Physics 107 (2010) 054105.

[22] M.J. Haun, E. Furman, S.J. Jang, L.E. Cross, Phenomenology, Ferroelectrics 99 (1989) 13–25.
[23] A. Ullah, C.W. Ahn., A. Hussain, S.Y. Lee, I.W. Kim, Phase transition, electrical properties, and temperature-insensitive large strain in $BiAlO_3$-Modified $Bi_{0.5}(Na_{0.75}K_{0.25})_{0.5}TiO_3$ lead-free piezoelectric ceramics, Journal of the American Ceramic Society 94 (2011) 3915–3921.
[24] T. Takenaka, H. Nagata, Y. Hiruma, Phase transition, temperatures and piezoelectric properties of $(Bi_{1/2}Na_{1/2})TiO_3$-and $(Bi_{1/2}K_{1/2})TiO_3$-based bismuth perovskite lead-free ferroelectric ceramics, IEEE Transactions on Ultrasonics, Ferroelectrics and Frequency Control 56 (2009) 1595–1612.
[25] B. -J. Chu, D.-R. Chen, G.-R. Li, Q.-R. Yin, Electrical properties of $Na_{1/2}Bi_{1/2}TiO_3$–$BaTiO_3$ ceramics, Journal of the European Ceramic Society 22 (2004) 2115–2121.
[26] Y.A. Boikov, D. Erts, T. Claeson, A.Y. Boikov, Dielectric response of $Ba_{0.75}Sr_{0.25}TiO_3$ epitaxial films to electric field and temperature, Physics of the Solid State 44 (2002) 2157–2164.
[27] H. Mostaghaci, R.J. Brook, Microstructure development and dielectric properties of fast-fired $BaTiO_3$ ceramics, Journal of Materials Science 21 (1986) 3575–3580.
[28] U. Skibbe, J.T. Christeller, P.T. Callaghan, C.D. Eccles, W.A. Laing, W. Cao, C.A. Randall, Grain size and domain size relations in bulk ceramic ferroelectric materials, Journal of Physics and Chemistry of Solids 57 (1996) 1499–1505.